

The extra-planar neutral gas in the edge-on spiral galaxy NGC 891

Filippo Fraternali

Theoretical Physics, University of Oxford (UK)

Tom Oosterloo

ASTRON, Dwingeloo (NL)

Renzo Sancisi

INAF-Bologna (I) & Kapteyn Institute, Groningen (NL)

Rob Swaters

Department of Astronomy, University of Maryland (MD)

Abstract. We present neutral hydrogen observations of the nearby edge-on spiral galaxy NGC 891 which show extended extra-planar emission up to distances of 15 kpc from the plane. 3D modeling of the galaxy shows that this emission comes from halo gas rotating more slowly than the gas in the disk. We derive the rotation curves of the gas above the plane and find a gradient in rotation velocity of $-15 \text{ km s}^{-1} \text{ kpc}^{-1}$. We also present preliminary results of a galactic fountain model applied to NGC 891.

1. Introduction

NGC 891 is one of the best known and studied nearby edge-on spiral galaxies. It is at the distance of 9.5 Mpc, is classified as a Sb/SBb, and it is often referred to as a galaxy very similar to the Milky Way (van der Kruit 1981). Because of its very high inclination ($i \geq 88.6^\circ$, Rupen 1991) it is very suitable for the study of the distribution and kinematics of the gas above the plane.

NGC 891 has been the subject of numerous studies at different wavelengths that have led to the detection of various halo components: an extended radio halo (Allen, Sancisi, & Baldwin 1978; Hummel et al 1991), an extended layer of diffuse ionised gas (DIG) (e.g. Dettmar 1990) and diffuse extra-planar hot gas (Bregman & Pildis 1994). Also “cold” ISM components have been detected in the halo such as H I (Swaters, Sancisi, & Van der Hulst 1997), dust (Howk & Savage 1999) and CO (Garcia-Burillo et al. 1992).

Here we concentrate on the neutral gas and present results from recent third generation H I observations obtained with the Westerbork Synthesis Radio Telescope (WSRT). NGC 891 was first studied in H I in the late seventies with the WSRT and the presence of neutral gas seen in projection out of the plane was reported (Sancisi & Allen 1979). Subsequently, a new study with higher

sensitivity showed that the extra-planar emission was very extended, up to 5 kpc from the plane. 3D modeling indicated that such emission was produced by a thick layer of neutral gas rotating more slowly than the gas in the disk (Swaters et al. 1997).

Since then, several other studies have confirmed the presence of neutral gas in the halos of spiral galaxies. It has been detected in edge-on or nearly edge-on systems (e.g. UGC 7321, Matthews & Wood (2003) and NGC 253, Boomsma et al. (2004)), as well as in galaxies viewed at different inclination angles (e.g. NGC 2403, Fraternali et al. 2001). Indications of vertical gradients in rotation velocity have been found in several galaxies also in the ionised gas (e.g. NGC 891, Pildis, Bregman, & Schombert (1994), Rand (1997); NGC 5055, Rand (2000)).

In the first part of the paper we present the new HI observations of NGC 891 together with a 3D modeling of the HI layer. In the second part (Section 3) we study the kinematics of the extra-planar gas and, in the third one (Section 4), we present results from a dynamical model of the extra-planar gas.

2. HI observations

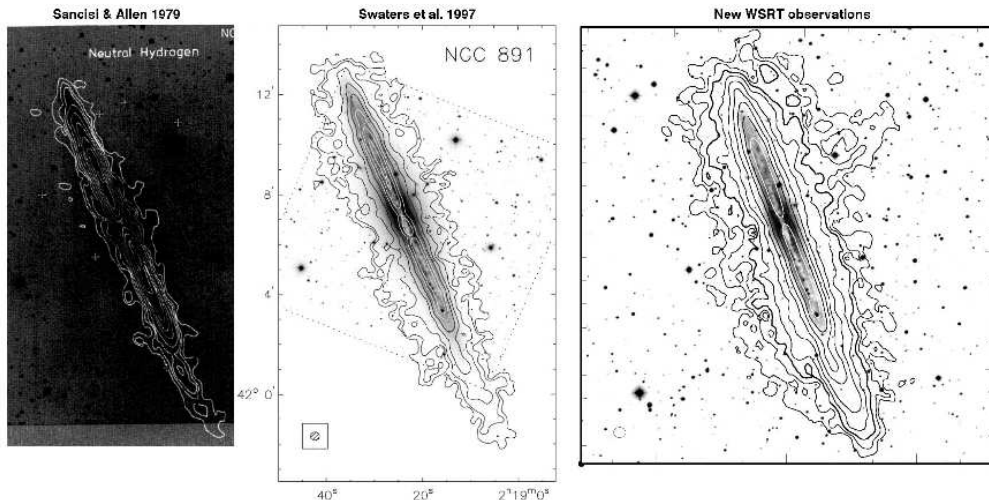


Figure 1. Total HI map of NGC 891 (right) obtained from our new WSRT observations compared with the total HI maps of the previous observations (Sancisi & Allen 1979; Swaters et al. 1997). Contours of the new total HI map are: $1.7, 4.5, 9, 18.5, 37, 74, 148, 296.5, 593 \times 10^{19}$ atoms cm^{-2} .

The new observations of NGC 891 have been carried out during the second semester of 2002 with the Westerbork Synthesis Radio Telescope (WSRT) and a total integration time of about 200 hrs. With this long integration time we reach a sensitivity (r.m.s. noise per channel = 0.22 mJy/beam at $28'' \times 16.5 \text{ km s}^{-1}$ resolution) that is about a factor 4 better than the previous observations of Swaters et al. (1997). A complete presentation of the observations will be given in Oosterloo et al. (in preparation).

Figure 1 (right panel) shows the new total HI map of NGC 891 at $28''$ (~ 1.3 kpc). HI emission is detected at a projected distance of as far as 15

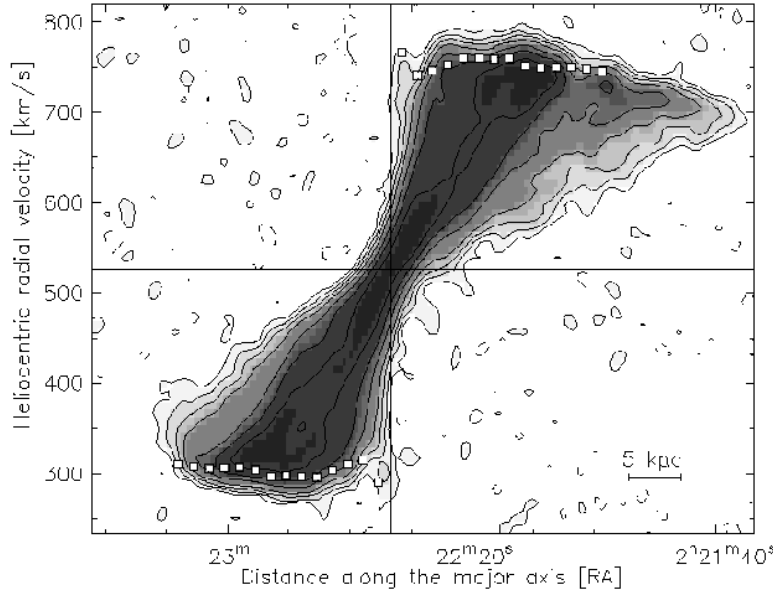


Figure 2. HI position-velocity diagram along the major axis of NGC 891. The white squares show the rotation curve derived using only the approaching side of the galaxy.

kpc from the plane (see the spur in the N-W side of the disk). The size of the disk itself (in the plane) is very similar to that reported by Swaters et al. (1997) and Sancisi & Allen (1979) suggesting that we have possibly reached the edge of the HI disk, especially on the N-E side. The emission above the plane, instead, is significantly more extended than in previous observations and almost everywhere extends up to 10 kpc above and below the plane.

Figure 2 shows the position-velocity plot along the major axis of NGC 891 at 28'' resolution with the rotation curve (white squares) overlaid. The rotation curve was derived with the method described in section 3 using only the N-E (approaching) side of the galaxy. The kinematics of the receding side within a radius of ~ 6 kpc is very similar to that of the approaching one. At larger radii the velocity is apparently declining. However, we cannot be sure that the gas in this extension is at the line of nodes and, therefore, the derivation of a rotation curve in that region is not possible. In the inner regions of the galaxy (about 1-2 kpc) we confirm the presence of a fast rotation disk or ring (see also Swaters et al. 1997).

2.1. The extra-planar gas

The total HI map of NGC 891 (Figure 1) shows extended emission in the direction perpendicular to the plane. Is this emission coming from gas located in the halo of the galaxy or is it the result of projection effects? Here we address this question using a 3D modeling technique similar to that of Swaters et al. (1997).

In Figure 3 we compare some of the observed channels maps of NGC 891 (right hand column) with models of the HI layer. From the left hand column they are: 1) a warp along the line of sight, i.e. a change of the inclination angle

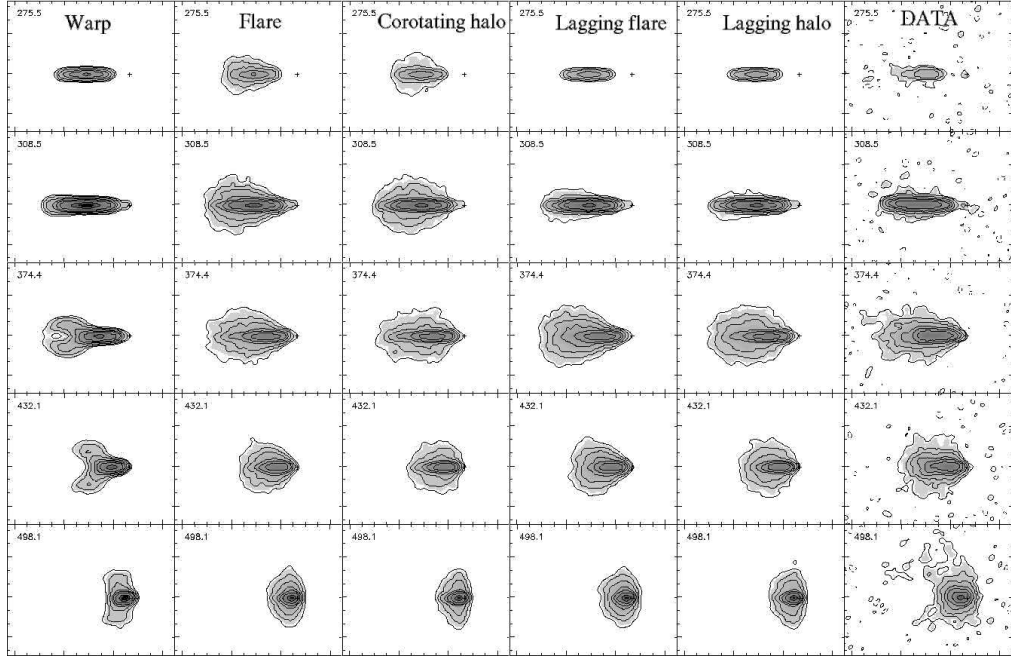


Figure 3. Channel maps for NGC 891 compared with galaxy models (see text).

of the disk, from 90 to 60 degrees, in the outer parts; 2) a flaring (increasing thickness) of the outer disk from a FWHM of 0.5 kpc up to \sim 6 kpc; 3) a two-component model with thin disk + thick (FWHM \sim 6 kpc) disk corotating; 4) and 5) two-component models with the thick disk rotating more slowly (35 km s^{-1}) than the disk. The models in columns 4 and 5 differ only for the radial density distribution of the thick component: one (5) is the same (scaled) as that of the gas in the disk and the other (4) has a depression in the central regions.

Of the models reported here, only those in columns 4 and 5 give a reasonable reproduction of the data. In particular the warp model does not reproduce the shape of channel maps at 374 and 432 km s^{-1} , while the flare and corotating model do not reproduce the thin channels of the two top rows (at 275.5 and 308.5 km s^{-1}). This clearly indicates that the extra-planar emission in NGC 891 is produced by a thick (FWHM \sim 6 kpc) layer of HI rotating more slowly than the gas in the plane. The halo is possibly relatively denser than the disk in the outer parts (with a radial density distribution somewhat in between the models in column 4 and 5).

3. Kinematics of the extra-planar gas

In the previous section we have presented some simple galaxy models showing that the emission above the plane in NGC 891 comes from gas which is located in the halo region and rotates more slowly (is lagging) with respect to the gas in

the plane. Here we quantify this lag by deriving the 2D rotation velocity field (rotation surface) or rotation curves at different heights from the plane.

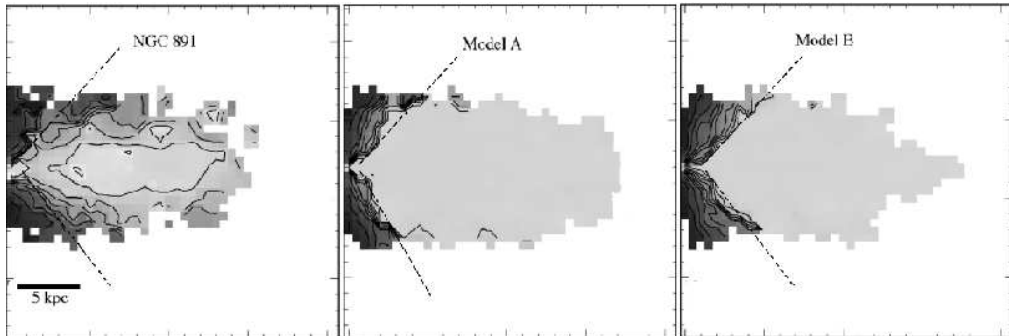


Figure 4. Rotation velocity surfaces for NGC 891 (N-E side) and two model galaxies obtained with the envelop-tracing technique. The centre of the galaxy is at the middle of the left edge of each figure. The models have constant rotation velocity in R and z . In the inner regions (outlined by the dashed lines) the envelop-tracing fit does not work properly (i.e. it does not return the input constant rotation velocity).

A rotation curve of a spiral galaxy seen edge-on is usually derived using an envelop-tracing method i.e. by taking the highest measured velocity along the line of sight as the rotation velocity (e.g. Sancisi & Allen 1979). This method was, for instance, used to derive the rotation curve shown in Figure 2. In an ideal situation (high S/N, galaxy perfectly edge-on, pure rotation, etc.) the highest velocity measured along the line of sight is indeed produced by the gas at the line of nodes (i.e. rotation velocity). However, the real situation can be very different. In particular it is possible that the emission from the gas at the line of nodes is below detection and, as a consequence, the rotation velocity is underestimated. This could easily happen when observing the gas above the plane where the density is lower and especially in cases of central H I depressions or holes.

Figure 4 (left panel) shows the rotation velocity surface (contours with constant v_ϕ) of NGC 891 derived with the envelop-tracing method for the N-E side of the galaxy. Can this rotation velocity field be fully trusted?

In order to test this, we have constructed model galaxies with known (flat) rotation velocity in R and z . Figure 4 (central and right panels) shows two rotation velocity surfaces obtained from two of these models. These surfaces are obtained using exactly the same fit and fitting parameters as for the one of NGC 891 (left panel). The two models have different radial density distributions for the extraplanar gas. These were obtained from the data from above (N-W side, Model A) and below (S-E side, Model B) the disk. The results show that the fit works very well in a large part of the galaxy giving a constant value of the velocity in R and z (uniform lowest gray level). The fit does not return the input constant rotation velocity with z only in the inner regions outlined by the dashed lines in Figure 4. There is very little difference between the results obtained with the two different radial density distributions. These results were

used to exclude the inner regions in the 2D rotation velocity field of NGC 891 (left panel).

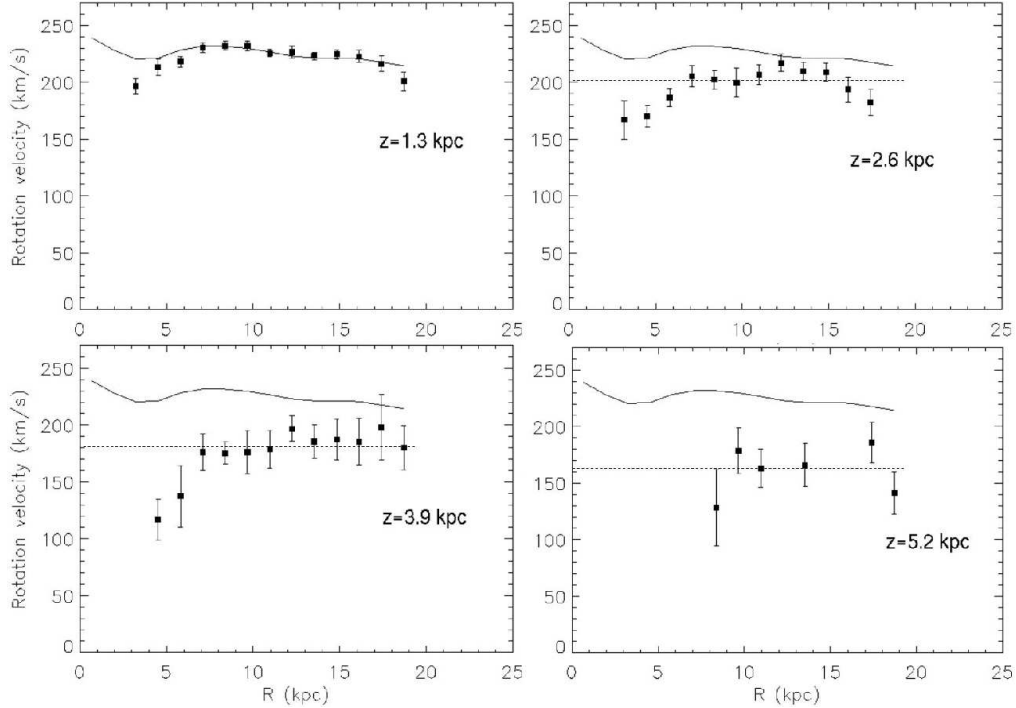


Figure 5. Rotation curves for NGC 891 at various distances from the plane. The solid line shows the rotation curve in the plane and the dashed lines outline the value of the flat part of the rotation curves. Only the N-E side of the galaxy has been used to derive these curves.

Figure 5 shows the results for NGC 891 plotted as rotation curves at various distances from the plane after the uncertain inner points have been removed. The solid line shows the (smoothed) rotation curve in the plane while the dashed lines outline the value of the flat part of the rotation curves at the different heights. The halo of NGC 891 appears to corotate up to 1.3 kpc, then it starts to lag with respect to the disk, the lagging increasing with height from the plane. Given the limited angular resolution, the apparent corotation below 1.3 kpc may be the effect of beam-smearing. The gradient in rotation velocity is roughly $15 \text{ km s}^{-1} \text{ kpc}^{-1}$. The West and East side of the galaxy do not show significant differences. A detailed description of this procedure and results will be given in a forthcoming paper (Fraternali, in preparation).

4. Dynamical models

The presence of neutral gas in the halo of spiral galaxies is still unexplained. It can be either the result of a galactic fountain (Shapiro & Field 1976) and/or of accretion from the intergalactic medium (e.g. Oort 1970). The processes involved are probably non-stationary and require a dynamical modeling of the

medium above the plane (see Barnabé et al. (2004) for a stationary model). As a first approach to the problem we have considered a ballistic (particle-based) model for the gas expelled from the plane as a result of star formation activity (see also Collins, Benjamin, & Rand 2002). We have considered a multicomponent potential with stellar and gaseous exponential disks, a $r^{1/4}$ bulge and a double power-law dark matter halo with adjustable flatness (in analogy to the galactic models of Dehnen & Binney 1998).

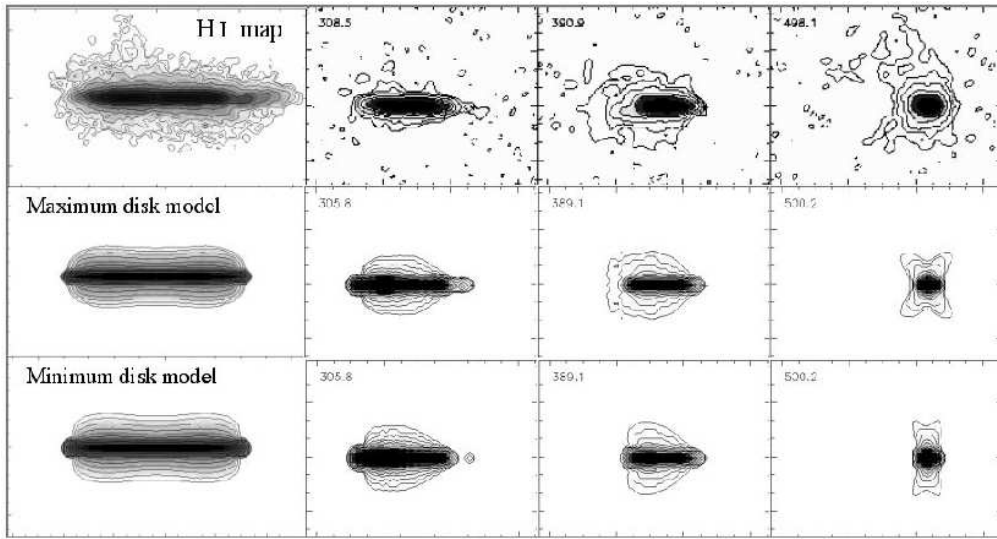


Figure 6. Total HI map and representative channel maps for NGC 891 (top) compared to two ballistic models of galactic fountains. The number in the upper left corners are heliocentric velocity (km s^{-1}).

A C++ code was written to integrate the orbits of the particles and project them along the line of sight. The particles are shot vertically with different kick velocities from 0 to a maximum v_{\max} that can depend on R . For each dt (time interval) the position and velocity of the particle is projected along the line of sight and the integration is carried out until the particle falls back to the plane. The output of the code is a model cube that can be compared with the data cubes. These models can be applied to external galaxies viewed at any inclination angle as well as to the Milky Way (internal projection). Here we show a preliminary application to NGC 891. Details and improvements of the model to take into account also non-ballistic effects and gas accretion from the intergalactic medium will be presented in a forthcoming paper (Fraternali & Binney, in preparation).

Figure 6 shows the total HI map and some representative channel maps for NGC 891, compared with the outputs of two ballistic models. The two models are for a maximum and a minimum disk fit of the rotation curve with B band M/L ratios of 7 and 1 respectively. The parameters of the models have been “tuned” to reproduce as well as possible the vertical distribution of the gas and the shape of the channel maps. This figure shows that both ballistic models can qualitatively reproduce the data. However, there seem to be problems in

reproducing the thinness of the channel maps around 300 km s^{-1} i.e. there is not enough lagging in the halo. This is not the effect of the potential considering that little differences are visible when considering extreme choices of the potential shape. This preliminary analysis suggests that the pure ballistic galactic fountain models fail to explain the amount of lagging in galactic halos and that other phenomena such as gas accretion may be important.

5. Conclusions

New HI observations of the edge-on spiral galaxy NGC 891 show the presence of extraplanar neutral gas up to distances of 15 kpc from the plane. We have used these data to derive, for the first time, a 2D rotation velocity field (in R and z) of an edge-on spiral galaxy. We find that the extra-planar gas is corotating with the gas in the disk up to about 1.3 kpc; beyond that it rotates more slowly by about $15 \text{ km s}^{-1} \text{ kpc}^{-1}$. Dynamical models of NGC 891 show that a pure ballistic galactic fountain can qualitatively reproduce the data. However, problems with missing low angular momentum material suggest that other mechanisms such as accretion may also play a role.

References

Allen, R.J., Sancisi, R., Baldwin, J.E. 1978, A&A, 62, 397
 Barnabé M., Ciotti L., Fraternali F., Sancisi R. 2004, this conference
 Bregman, J.N. 1980, ApJ, 236, 577
 Bregman, J.N., Pildis, R.A. 1994, ApJ, 420, 570
 Boomsma, R., Oosterloo T., Fraternali F., van der Hulst J.M., Sancisi R. 2004, A&A, accepted
 Collins, J.A., Benjamin, R.A., Rand, R.J. 2002, ApJ, 578, 98
 Dehnen, W., Binney, J. 2001, MNRAS, 294 429
 Dettmar, R.J. 1990, A&A, 232, L15
 Garcia-Burillo, S., Guelin, M., Cernicharo, J., Dahlem, M. 1992, A&A, 266, 21
 Fraternali, F., Oosterloo, T., Sancisi, R., Van Moorsel, G., 2001, ApJ, 562, L47
 Fraternali, F., Oosterloo, T., Boomsma R., Swaters R., Sancisi R. 2003, "Recycling Intergalactic and Interstellar Matter", IAU, Symposium no. 217, 44
 Howk, J.C., Savage, B.D. 1999, AJ, 117, 2077
 van der Hulst, T., Sancisi, R. 1988, AJ, 95, 1354
 Hummel, E., Dahlem, M., van der Hulst, J.M., Sukumar, S. 1991, A&A, 246, 10
 van der Kruit, P.C. L. 1981, A&A, 99, 298
 van der Kruit, P.C., Searle, L. 1981, A&A, 95, 105
 Matthews, L.D., Wood, K. 2003, ApJ, 593, 721
 Oort, J.H. 1970, A&A, 7, 381
 Pildis A.R., Bregman J.N., Schombert J.M. 1994, ApJ, 423, 190
 Rand, R.J. 1997, ApJ, 474, 129
 Rand, R.J. 2000, ApJ, 537, L13
 Rupen, M.P. 1991, AJ, 102, 48
 1979, A&A, 74, 73
 Shapiro, P.R., & Field G.B. 1976, ApJ, 205, 762
 Sofue, Y., Rubin, V. 2001, ARA&A, 39, 137
 Swaters, R.A., Sancisi, R., & van der Hulst, J.M. 1997, ApJ, 491, 140
 Wakker, B.P., & van Woerden H. 1997, ARA&A, 35, 217